https://doi.org/10.1016/j.atmosenv.2020.118044

A novel semi-automatic method for measuring acidic ultrafine particles in the atmosphere

Haoxian Lu, Xiaopu Lyu, Hai Guo*

Air Quality Studies, Department of Civil and Environmental Engineering, The Hong Kong Polytechnic University, Hong Kong, China

*Corresponding author. ceguohai@polyu.edu.hk

Abstract

The adverse effects of acidic ultrafine particles (AUFPs) have been widely recognized in scientific communities. Two methods have previously been developed to measure AUFPs, but there are certain drawbacks. Thus, the aim of the study was to develop an easier, more rapid and more accurate measurement system for semi-automatic measurement of AUFPs in the atmosphere. The new measurement system was developed by integrating a diffusion sampler (DS) with three quartz crystal microbalances (QCM), namely QCM+DS system. The QCM detectors were coated with a nano-film of metal (metal-QCM detectors) and then placed inside the DS at three sampling spots for collection and detection of ultrafine particles (UFPs). The frequency changes obtained from the metal-QCM detectors were converted into the weights of deposited particles and used to determine the proportions of AUFPs in UFPs through the removal process of non-AUFP particles. Prior to sampling, the sensitive response of the QCM system and collection efficiencies of the QCM+DS system were calibrated using standard acidic and non-acidic particles. Reactions between the AUFPs and nano-film of metal were guaranteed by confirming much lower than one-layer deposition of particles on the detectors based on theoretical calculation and experimental results. Finally, the QCM+DS system was validated in a field measurement by comparing the results with those obtained from the previously developed method and a commercial measurement system (*i.e.* SMPS). All the three methods showed good agreements in measuring AUFPs and UFPs concentrations, indicating the reliability of the QCM+DS system for the quantification of ambient UFPs and AUFPs.

Key words: Semi-automatic; Acidic Ultrafine Particles (AUFPs); QCM+DS; Nano-film of metal

1. Introduction

Accumulated evidence strongly suggests that the number of acidic ultrafine particles (AUFPs) is more closely correlated with total mortality, morbidity and hospital admissions for respiratory diseases (Thurston et al., 1989, 1992, 1994; Lippmann and Thurston, 1996; Peters et al., 1997; Wichmann et al., 2000; Cohen et al., 2000). In addition to health issues, AUFPs have impacts on climate, visibility and secondary organic aerosol (SOA) production (Kim et al., 1994; Li et al., 2010). Hence, it is critical to be able to distinguish AUFPs from the total number of ultrafine particles (UFPs), and to quantify the number concentrations of AUFPs in the atmosphere. Only with this information can effective control measures be formulated and implemented. However, no reliable measurement techniques were available to obtain the number concentrations of AUFPs until 2012, as earlier methods can only identify the AUFPs in the atmosphere, but cannot quantify them (Wang et al., 2012; Cohen et al., 2004). Two methods were developed by our group in 2012 and 2014, respectively, to measure the AUFPs in the atmosphere with the nano-film detectors (*i.e.* ESP+AFM and DS+AFM, respectively) (Wang et al., 2012, 2014). In the previous methods, nano-film detector was generated by using the magnetron sputtering system to coat a 25 nm metallic film on a silicon wafer. Afterwards, the detectors were deployed in the electrostatic precipitator (ESP) and/or diffusion sampler (DS) for the collection of UFPs in the atmosphere. Unlike non-acidic UFPs, AUFPs deposited on the detectors caused reaction spots, which were examined by an Atomic Force Microscopy (AFM) to distinguish AUFPs from non-acidic UFPs and measure their sizes. Thus, enumeration and size measurement of AUFPs were achieved according to the number and diameter of particles deposited on the detectors after considering the scanning area, collection efficiency and sampling duration. Both methods proved that nano-film detector was a reliable method to differentiate AUFPs from UFPs and to quantify AUFPs.

Although the above methods can be used to quantify the concentration of AUFPs, the fact is that these methods are offline and require enormous resources to support AFM analysis. The AFM is a widely used technique in aerosol studies due to its high imaging resolution (1 nm in lateral and 0.1 nm in vertical) and few limitations (Heath et al., 2018). The AFM operation does not require special environment (*e.g.* vacuum and high/low temperature) and sample pre-treatments. However, the AFM instrument is neither inexpensive nor compact, nor easy to operate, which hinders its wide application

in field measurements. Moreover, as a manual instrument, AFM analysis is highly time-consuming. Numerous AFM scans are required to reduce the uncertainty caused by incomplete scanning of the entire detector. Thus, it is impractical to obtain vast amounts of AUFPs data using the previous methods. It is necessary to improve/revise the previous methods so that AUFPs can be enumerated and sized online after collection on a nano-film detector without using AFM.

This study developed a novel method for semi-automatic measurement of AUFPs in the atmosphere, named QCM+DS. Here, the semi-automatic means "partly operated by machinery, not human". The QCM+DS system was developed by integrating the previous DS with quartz crystal microbalances (QCM). The QCM is an extremely sensitive online mass sensor with a detection capacity in the sub-nanogram range (Ward and Buttry, 1990; McCallum, 1989, Chen et al., 2016). Noteworthily, the linear relationship of QCM response with mass is only applicable to uniform, rigid and/or thin-film deposition (Buttry, 1991). In the case of depositing soft polymers or biomolecules, the relationship between mass and frequency may be destroyed. Owing to its high sensitivity, fast response and real-time detection capabilities, QCM offers the opportunity to improve the previous DS and nano-film detectors. By functionalizing the surface of the QCM detector with a nano-film of metal, QCM could use its real-time measurement capabilities to monitor the temporal variations of ambient AUFPs. That is, deployment of the coated QCM detectors inside the DS would enable us to conduct long-term online measurements. Prior to sampling, the sensitive response of the QCM system and the collection efficiencies of the QCM+DS system were calibrated using standard acidic and non-acidic particles. Reactions between the AUFPs and nano-film detectors were guaranteed by confirming much lower than one-layer deposition of particles on the detectors. After calibration, the QCM+DS system was deployed in an outdoor measurement together with the previous DS+AFM method and a commercial instrument (*i.e.* Scanning Mobility Particle Sizer (SMPS)) for method validation.

2. Materials and Methods

2.1 Quartz Crystal Microbalance (QCM)

A quartz crystal microbalance (QCM) measures a mass variation per unit area by detecting the change in frequency of a detector. The resonance is disturbed by the addition or removal of a slight mass.

High-precision (0.01 Hz) and high-resolution frequency (1 second) measurements are readily made. As a gravimetric instrument, the QCM measures mass ranging from micrograms to fractions of a nanogram. Its detection limits correspond to sub-monolayers of atoms. The changes in resonant frequency are used as a direct measurement of mass changes on the surface of the QCM according to the Sauerbrey's equation (Eq. 1), which is shown below,

$$\Delta f = -K \cdot \Delta m \qquad \text{Eq. 1}$$

where Δf is the measured frequency change in Hz, K is the sensitivity factor for the detector in $Hz \cdot cm^2/\mu g$, and Δm is the change in mass per unit area in $\mu g/cm^2$. Hence, if the QCM is used for the collection of particulate matters (PM), the mass change can be readily detected. In this study, three QCM systems (QCM200, Stanford Research Systems) were adopted and integrated with the previous DS to develop a new sampler, *i.e.* QCM+DS. The purpose of using three QCM systems was to understand the collection efficiency at different distances from the inlet. The QCM200 system includes a controller, crystal oscillator electronics, a crystal holder and detectors.

2.2 Metal-QCM detectors

Magnetron sputtering system (MSS) was proved to be a proper method for coating a nano-film of metal on the surface of substrate (Wang et al., 2012). The surface of the MSS coating and the adhesion to the substrate remains stable under severe weather condition. Thus, the MSS was adopted in this study to coat the nano-film of metal on the surface of the QCM detector, forming metal-QCM detectors. Using the MSS, a nanostructure interface of the metal was fabricated by ejecting the metal atoms onto the surface of the detector under high-voltage bombardment. It was proved that the nano-film of metal reacted with the deposited AUFPs. Pure QCM detector was firstly ultrasonically cleaned in sulfuric acid solvent (2 mol/L), ethanol and purified water, respectively, to remove all the fine particles and impurities on its surface. A plate was used to place the detector before and after sputtering to prevent contamination. The base pressure of the chamber was lower than 4×10^{-5} Torr before MS deposition and the total pressure for sputtering was kept at 1.3×10^{-2} Torr. In an ultrahigh vacuum environment, metal target was activated at a high voltage of ~400 volts to produce plasma and then sputtered metallic atom on the surface of the QCM detectors. To obtain ~25 nm thickness of metallic film, sputtering

duration of 2.5 min was adopted. After sputtering, the metal-QCM detectors were stored in a nitrogen atmosphere to avoid oxidation of the nano-film surface.

2.3 Fabrication of the QCM+DS system

The developed QCM+DS system was fabricated by integrating the previous DS with three QCMs. Introduction of the previous DS was described in previous study (Wang et al., 2014). To integrate the QCMs with the DS, modification was made, including the inlet and the sampling spots. Details of the modification are narrated in the supplement (Text S1).

The schematic diagram of the QCM+DS system is shown in Fig. 1. Specifically, 1 is the inlet unit (Fig. S1 for detail). 2 is the rubber used to seal the sampler. 3 is the metal-QCM detector which is put inside the system. 4 is the channel for collecting air sampler. 5 is the outlet of the sampler. 6 is the inlet tube for connecting with a dryer outside. 7 is the upper panel of the diffusion sampler. 8 is the installation groove which can suitably place the detector. 9 are the two QCM pins which enable the connection between the detector and digital controller. 10 is the QCM digital controller. A is the sampling spot inside the QCM+DS system. Sectional view of A is also displayed in Fig. 1. In particular, the locations of the three sampling spots (*i.e.* spot A, spot B and spot C) were at 85.0, 201.5, and 472.5 mm (midpoint of the rectangular recess) from the inlet along the length of the channel, respectively (Fig. S2 for detail). The L1, L2, L3, L4, and L5, L6 were the distances of left and right sides of metal-QCM detectors from the inlet at the three locations, respectively. Details of the particle collection procedure in the QCM+DS system were narrated in Text S2.

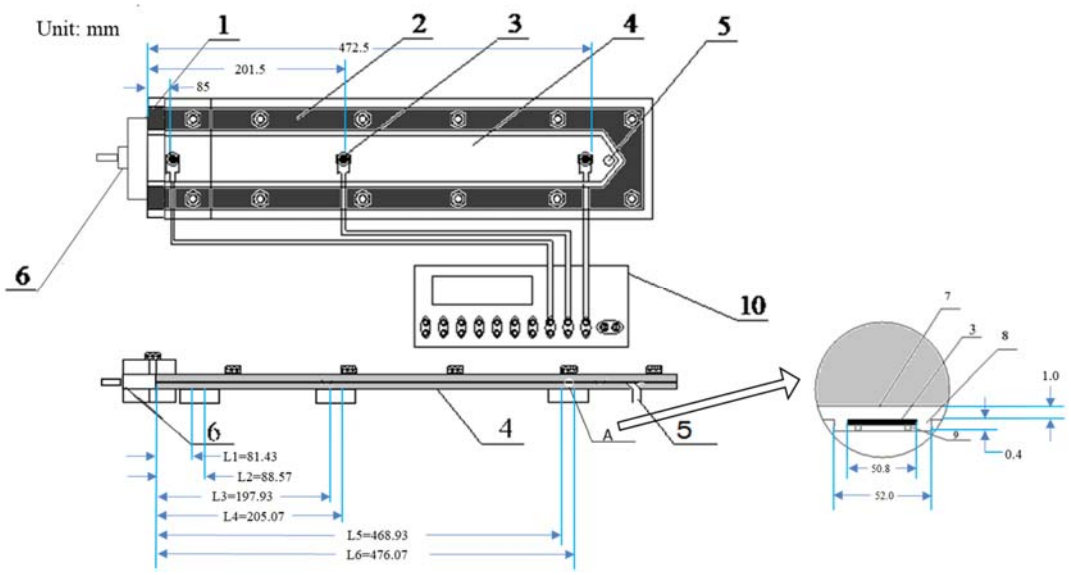

Fig. 1 Schematic diagram of the QCM+DS system

2.4 Calibration of the QCM+DS system

2.4.1 Calibration of sensitivity factor of the QCM

The Sauerbrey's equation relies on a linear sensitivity factor, K, which is a fundamental property of the QCM. Sauerbrey's equation is only strictly applicable to uniform, rigid, thin-film deposits (Buttry, 1991). As the QCM detector was modified (section 2.2) and different sizes of particles would be measured in this study, calibration of the sensitivity factor of the QCM after modification was needed.

Both standard acidic and non-acidic particles were used to calibrate the sensitivity factor to avoid the influence of reactions between the acidic particles and the nano-film of metal. A calibration system was set up using standard non-acidic particles (Fig. S3). The system comprised a particle generation unit, a particle collection unit and a condensation particle counter (CPC; Model 5.400, Grimm, Germany). In the particle generation unit, a particle generator (Model 7.811, Grimm, Germany) was used to generate standard non-acidic particles of polystyrene latex spheres (PSL) (Thermo Scientific, USA) and sodium chloride. After generation, particles passed through a dilution bottle and a silicone gel dryer to buffer and remove water vapor, respectively. The particle collection unit included an ESP with metal-QCM detectors inside. In our system, the ESP was used to collect the generated particles and the collection efficiency of the ESP was 100% for particles smaller than 200 nm (Wang et al.,

2012). A differential mobility analyzer (DMA) was used to select monodisperse particles for follow-up collection. After size selection, particles were collected on a metal-QCM detector mounted in the ESP at a flow rate of 0.3 l/min. Frequency change of the metal-QCM detector was obtained after a certain sampling time. A CPC measured particle number concentration simultaneously during the calibration process at the same flow rate as ESP (*i.e.* 0.3 l/min). As for the calibration system using standard acidic particles, the particle collection unit and the CPC were the same, while the particle generation unit was altered to a standard acidic particle generation (SAPG) system (Fig. S4). Details of the SAPG system were described in our previous study (Wang et al., 2014).

The mass of deposited particles measured by the QCM system was compared with the particle number concentrations derived from the CPC. By considering densities and sizes of particles and sample volume, number concentrations derived from CPC were used to calculate the mass of deposited particles and the K value was then calibrated (Sarangi et al., 2016; Franken et al., 2019). Details are shown in Eq. 2 and Eq. 3.

$$\Delta m = C_{num} \cdot Q \cdot T \cdot (\frac{4}{3}\pi r^3 \cdot \rho) \quad \text{Eq. 2}$$

$$K = \frac{-\Delta f \cdot A}{C_{num} \cdot Q \cdot T \cdot (\frac{4}{3}\pi r^3 \cdot \rho)} \quad \text{Eq. 3}$$

where C_{num} is the number concentration of particles derived from CPC (count/cm^3), Q is the flow rate (cm^3/min), T is the sampling time (min), ρ and r are the density (g/cm^3) and radium (cm) of particles, and A is the area of the metal-QCM detector (cm^2), respectively.

2.4.2 Calibration of collection efficiency of the QCM+DS system

As a modified diffusion sampler, the collection efficiency is dependent upon the theory of diffusion presented by Hinds (1999), which is related to the deposition parameter (μ). The deposition parameter (μ) is determined by Eq. 4 and Eq. 5.

$$\mu = \frac{D \times L \times W}{Q \times h} \quad \text{Eq. 4}$$

$$D = \frac{\mathrm{k} \times \mathrm{T} \times \mathrm{C_c} \times 10^{10}}{3\pi \times \gamma \times \mathrm{d_p}} \quad \text{Eq. 5}$$

where μ is the deposition parameter, L is channel length (cm), W is channel width (cm), Q is flow

rate (cm^3/sec), and h is channel height (cm), D is the diffusion coefficient of the particle (cm^2/sec) and determined by the Stokes-Einstein equation (Eq. 5), where k is Boltzmann's constant (1.38×10^{-23} J/K), T is the absolute temperature, C_c is the slip correction factor, γ is the air viscosity (1.79×10^{-6} Pa·sec), and d_p is the particle diameter (mm).

Collection efficiencies of particles in the QCM+DS system were calibrated using three sizes of PSL particles (53 nm, 102 nm and 200 nm) at four different sampling flow rates (0.05, 0.1, 0.2 and 0.5 l/min). In total, 12 experimental scenarios were conducted at each sampling spot. The schematic of calibration experiment setup is illustrated in Fig. S5. Two to three drops of PSL standards in each size were added into 8 mL Milli-Q water to generate PSL-particle aqueous solutions. The PSL particles, generated by the particle generator and diluted with filtered air using a 1.5 L bottle, were dried by a silica gel dryer (70 cm length×15 cm diameter), and then introduced into an environmental chamber. Every 2h, 5 mL PSL-particle aqueous solution was added into the particle generator to keep the generated aerosol at a stable level of about 10^3–10^4/cm^3, *i.e.* ~1.0×10^4/cm^3 for 50 nm, 4.0×10^3/cm^3 for 102 nm, and 2.0×10^3/cm^3 for 200 nm PSL particles. The chamber size was 70 (H)×60 (W)×90 (L) cm. The QCM+DS system was placed in the centre of chamber (Fig. S5). During the experiments, the frequency change of the system was recorded. To obtain sufficient frequency change for statistical analysis, totally 8~12 hours were required for sampling PSL aerosols. Simultaneously, a SMPS (DMA+CPC; Model 5.400, Grimm, Germany) measured the concentrations of monodisperse PSL aerosols inside the chamber every 4 mins throughout the entire experimental period. Eventually, the overall frequency change (Δf) was converted into the mass of deposited particles, which was compared with the total mass of particles passing through the QCM+DS system, measured by the SMPS. Thus, the collection efficiencies of the system on the three sizes of particles at four different sampling flow rates were obtained. The relationship of collection efficiencies of the QCM-DS system with sizes of particles and sampling flow rates was then quantified using the above experimental data (Origin Pro 2017, USA).

2.5 Particles removal process

To measure AUFPs, the key step is to differentiate acidic particles from non-acidic particles on the surface of the metal-QCM detector. In this study, ultrasonic method was adopted to remove non-acidic

particles on the nano-film detector without reactions (Wang et al., 2019). Specifically, non-acidic particles (*e.g.* NaCl particles) and acidic particles were generated and collected on the metal-QCM detectors, which were then treated by the ultrasonic. The acidic particles would react with the metal nano-film and form unique reaction spots, while non-acidic particles simply adhered to the surface without any reaction (Wang et al., 2012). Thus, non-acidic particles were removed from the surface based on the principle that the attractive forces between acidic particles and metal nano-film were different from those between non-acidic particles and metal nano-film. The non-acidic particles, *i.e.* NaCl aerosols, were generated using the particle generator, while the acidic particles were generated using the SAPG system. After collection of both non-acidic and acidic particles, metal-QCM detectors were transported to a beaker and then immersed in ethanol and sonicated/agitated at a high frequency (about 40 kHz) for 30 mins. The tapping mode of an AFM (NanoScope, Version 5.31R1, Veeco Instrument Inc., USA) was used to examine the workability of the ultrasonic method and determine the removal efficiency of particles before and after the treatment.

2.6 Validation via a field measurement

2.6.1 Sampling site

To validate the QCM+DS system, a field measurement was conducted from 11th April to 25th April 2019 at an urban site (Fig. S6). The site was on the rooftop of a building in the Hong Kong Polytechnic University. This site was significantly affected by anthropogenic emissions as it was located near busy roads and surrounded by residential areas.

2.6.2 Sampling technique and setup

Several instruments were employed in the field measurement, including the QCM+DS system, the previous DS and a SMPS (Model 5.400, Grimm, Germany). Results obtained from the previous DS+AFM method and SMPS were compared with those of the QCM+DS system. Schematic of the setup of sampling system is shown in Fig. S7. Ultrafine particles (UFPs) passing through the PM_1 cyclone were divided into two streams. The first stream went into the previous DS directly and particles were collected on the nano-film detectors. The other stream was further divided into two sub-streams. One sub-stream went through a DMA firstly for size selection to obtain monodisperse particles.

Afterwards, the monodisperse particles were collected by the QCM+DS system. The other sub-stream after the DMA was delivered to a CPC to monitor the number concentrations of UFPs. During sampling, both QCM+DS system and CPC measured the time-integrated size-resolved concentrations of ambient particles with a range of 5.5–150 nm at a 120-min scan interval. The QCM+DS system with three metal-QCM detectors inside continuously measured the mass of deposited particles (via frequency changes) at a flow of 0.1 L/min for 2 days for each sample, while the SMPS monitored size-classified particle number concentrations at a fixed flow rate of 0.3 L/min. At the end of each sampling, a HEPA filter was connected to the inlet of the QCM+DS to conduct blank experiment for at least 3 hours. On one hand, the blank experiment measured the frequency change when particle-free air was collected, which was considered in the data analyses. On the other hand, the system was cleaned by the particle-free air before the next sampling. For the previous DS, nine nano-film detectors were placed inside it for exposure. Ambient air was drawn through the sampler by a low-flow pump with a fixed flow rate of 0.05 L/min. Sampling duration of each sample was 2-4 days, dependent on the level of particle number in the air. Noteworthily, although the sampling was non-isokinetic, the measurement of ultrafine particles in the study was not affected (Arouca et al., 2010; https://www.ldxsolutions.com /particulate-matter-isokinetic-sampling/).

2.6.3 Data processing

After the field measurement, results obtained from the QCM+DS system were compared with those measured by the DS+AFM method and SMPS. The DS+AFM method was described in previous studies (Wang et al., 2012, 2014). The SMPS is a commercial instrument, which is able to measure number concentrations of UFPs online (maximum time resolution of 4 mins). As for the new QCM+DS system, real-time frequency of metal-QCM detector was obtained during sampling. To determine concentrations of UFPs in the atmopshere, frequency changes were converted into the masses of the deposited particles. By taking into account the collection efficiency, sampling flow rate and sampling duration, the concentrations of AUFPs and UFPs were determined. Specifically, in the QCM+DS system, particles ranged from 5.5 nm to 150 nm were categorized into 8 size bins (124~150 nm, 75~112 nm, 47~69 nm, 30~43 nm, 19~27 nm, 17~12 nm, 11~8 nm, and 7~5 nm) in one scanning interval (*i.e.* 2 hours) for calculation and comparison with the results of SMPS and DS+AFM method. Frequency

change of one size bin corresponded to the sampling duration (15 mins) in one scanning interval. However, due to the tiny frequncy change in the smaller size bins (*i.e.* 17~12 nm, 11~8 nm and 7~5 nm), the three size bins were merged into one category for calculation (*i.e.* 17~5 nm). In collecting one sample, sampling duration of the QCM+DS system was 2 days. Thus, sum of frequency changes for each size bin in one sample was used to calculate the particle concentraions in the 2 days. Eq. 6 explains the details of quantifying the concentrations of UFPs (C_m) using the QCM+DS system.

$$C_m=(\sum m_i/\eta_i)/(Q\times T) \quad \text{Eq. 6}$$

where C_m is the mass concentration of UFPs in the atmosphere; m_i is the mass of particles in i^{th} size bin, calculated using the Sauerbrey's equation (Eq. 1); η_i is the corresponding collection efficiency of particles in i^{th} size bin; Q is the sampling flow rate; T is the sampling time. Moreover, to convert mass concentration into number concentration, the density of ambient particles was assumed to be 2.5 g/cm^3 (Ferro et al., 2004; Cha and Olofsson, 2018). The conversion equation is as follows (Eq. 7).

$$n_i= m_i/(4/3\times\pi\times r_i^3\times\rho) \quad \text{Eq. 7}$$

where n_i is the total number of particles in i^{th} size bin; m_i is the mass of particles in i^{th} size bin; ρ is the particle density and r_i is the average radius of particles in the i^{th} size bin. Therefore, the total number concentration of UFPs (C_n) is further determined (Eq. 8).

$$C_n=(\sum n_i/\eta_i)/(Q\times T) \quad \text{Eq. 8}$$

Furthermore, to determine the concentrations of AUFPs, sampled metal-QCM detectors were immersed in the ethanol solution for ultrasonic treatment for 30 min after a certain storage time (longer than one day) in the inert gas. The storage time was to ensure a sufficient reaction between acidic particles and metal nano-film (Wang et al., 2012). Frequency changes before and after ultrasonic treatment were obtained. Frequency change after ultrasonic treatment was corresponded to the mass of non-acidic particles collected, while the frequency change in the field measurement referred to the mass of total UFPs. Thus, the mass of AUFPs was determined by the difference between the frequency changes in the field measurement and those after the ultrasonic treatment.

3. Results and Discussion

3.1 Sensitivity factor of QCM

3.1.1 Calibration of sensitivity factor using non-acidic particles

Fig. 2 shows the calibrations of sensitivity factor of the QCM system using non-acidic particles with sizes of 32 nm, 53 nm and 102 nm. The mass of deposited particles per unit area of each sample acquired from the CPC was plotted against the frequency changes measured by the QCM system. The slope for each size of particles was the sensitivity factor according to Eq. 3. The surface area of the quartz crystal (A) was equal to 0.4 cm^2. Particles of 102 nm and 53 nm were PSL particles while 32 nm particles were sodium chloride as the particle generator was unable to generate high enough concentrations of 32 nm PSL particles for collection. The densities of PSL and sodium chloride were 1.05 and 2.08 g/cm^3, respectively. Hence, the calibrated K value was 52.23 ± 4.90 $Hz \cdot cm^2/\mu g$ (R^2=0.99) for 102 nm particles, 59.83 ± 6.64 $Hz \cdot cm^2/\mu g$ (R^2=0.99) for 52 nm particles and 52.80 ± 8.49 $Hz \cdot cm^2/\mu g$ (R^2=0.99) for 32 nm particles. It can be seen that the calibrated K values were similar to the initial value of 56.6 $Hz \cdot cm^2/\mu g$ with a deviation of 3.0% set by the manufactory.

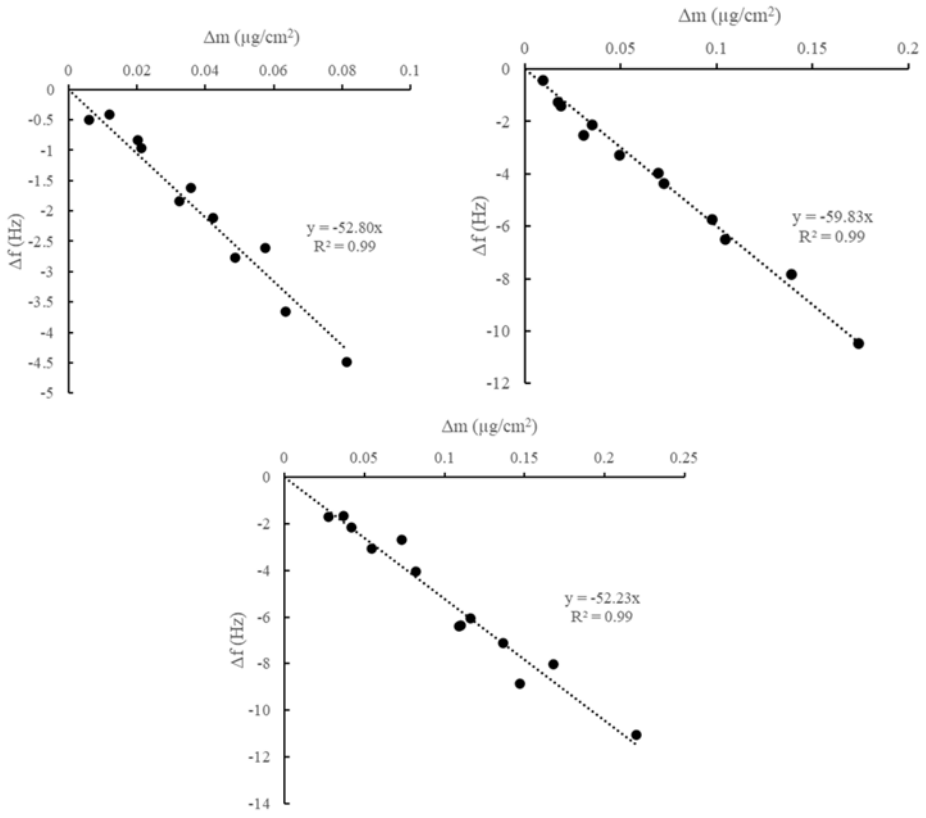

Fig. 2 Calibrations of sensitivity factors of the QCM system using different sizes of non-acidic particles (upper left panel: 32 nm; upper right panel: 53 nm; and lower panel: 102 nm)

3.1.2 Calibration of sensitivity factor using acidic particles

The calibration of sensitivity factor using acidic particles was similar to that using non-acidic particles. The same three sizes of acidic particles were generated and collected by both QCM+DS system and CPC. The density of acidic particles was determined as follows. Because the density of ultrafine carbon black particles was 0.55 g/cm^3 (Gilmour et al., 2004), and sulfuric acid accounted for 44.5%, 27.8% and 14.3% of the mass of 32 nm, 53 nm and 102 nm acidic particles, respectively (Zhang et al., 2008), the density of 102 nm acidic particle was estimated to be 0.73 g/cm^3 (*i.e.* ρ=0.55×(1-14.3%)+1.8×14.3%=0.73 g/cm^3). Likewise, the density of 32 nm and 53 nm acidic particles was 1.11 g/cm^3 and 0.90 g/cm^3, respectively. The calibration results are shown in Fig. 3. The calibrated sensitivity factors were 53.97 ± 6.07 Hz·cm^2/μg (R^2=0.96), 57.84 ± 17.98 Hz·cm^2/μg (R^2=0.95) and 59.13 ± 14.17 Hz·cm^2/μg (R^2=0.96) for 32 nm, 53 nm and 102 nm acidic particles, respectively. It can be seen that the results were similar to those of non-acidic particles and the initial value set by the manufactory. The R^2 were not as high (0.95-0.96) as those for non-acidic particles due to the fluctuation of the SAPG system. Overall, the acidic and non-acidic particles produced the same responses on the QCM system, and the initial value of sensitivity factor did not change after modification. Thus, the initial K value set by the manufactory was still adopted (*i.e.* 56.6 Hz·cm^2/μg) in the QCM+DS system in this study.

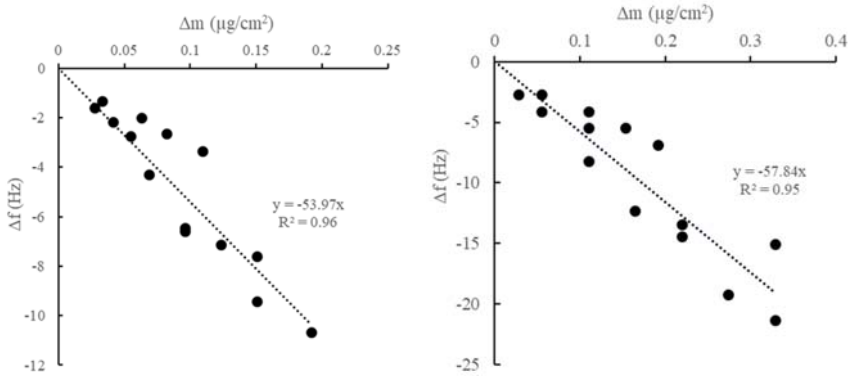

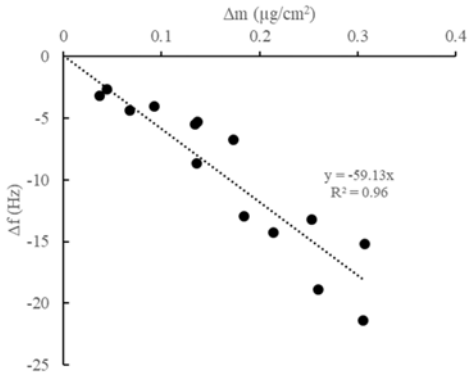

Fig. 3 Calibrations of sensitivity factors of the QCM system using different sizes of acidic particles (upper left panel: 32 nm: upper right panel: 53 nm; lower panel: 102 nm)

3.2 Confirmation of less than one-layer deposition

There were two issues about the feasibility of the QCM application into the DS for the measurement of acidic ultrafine particles. One was the recognizability of acidic particles by the QCM system and the other was the mass sensitivity of the QCM system. To distinguish the acidic particles, the deposition of particles was required to strictly fulfil single-layer coverage on the surface of the metal-QCM detectors in order to cause reactions between a single acidic particle and the coated detector. The maximum frequency change of the QCM system (*i.e.* Δf_{max}) during sampling was reached after a single-layer of closely-spaced particles was deposited on the surface. However, in practice, it was impossible to fully obtain/fulfil single-layer coverage of particles on the surface, not to mention the detection of a single-layer deposition. As such, the deposition of particles needed to be far less than single-layer coverage during sampling to avoid particles stacking. Meanwhile, it was essential to ensure that enough frequency change (*i.e.* Δf_{enough}, > 10 times the detection limit) could be detected in the case of a far less than single-layer deposition based on theoretical calculation (Shrivastava et al., 2011). There were some assumptions in theoretical calculation for Δf_{enough}: i) the coverage rate of particles was twentieth (*i.e.* 0.05); ii) the particles deposited on the surface had the same diameter; and iii) the average density of particle was $\rho = 2.5$ g/cm^3 (Ferro et al., 2004; Cha and Olofsson, 2018). The surface area of the quartz crystal $A = 0.4$ cm^2. For close-space arrangement of the particles, the surface usage rate $\lambda \approx 0.9$ according to geometry (Binks et al., 2017). Therefore, the particle number (N) for twentieth coverage rate of single-layer deposition $N = 0.05 \cdot \lambda A/s = 0.05 \cdot \lambda A/\pi r^2$. The s is the cross-

sectional area of the particle and r is the geometrical radius of the particle. The mass of a single particle $m = V\rho = 4\pi\rho r^3/3$. Thus, the total mass $M = Nm = 0.05 \cdot 4\rho r\lambda A/3$. As the relationship of frequency change with the mass of particles deposited on the surface followed the Sauerbrey's equation (Eq. 1), the theoretical Δf_{enough} for different sizes of particles (*i.e.* 5-350 nm) were calculated. The frequency changes of 5% coverage for single-layer deposition of particles ranged from 2.1 Hz to 148.6 Hz for 5 nm and 350 nm particles, respectively (Fig. S8). In theory, the highest resolution of the QCM system to detect frequency change is able to reach 0.01 Hz, which is significantly lower than the frequency change presented in Fig. S8, regardless of particle sizes. In conclusion, sufficient frequency change could be obtained even in the case of a far less than single-layer deposition of particles. Even so, it was still necessary to confirm that particles stacking would not occur under the circumstance of much lower than 100% coverage for single-layer deposition of particles. Otherwise, some acidic particles might stack upon others and could not react with the coated detector.

To confirm the hypothesis, polydisperse sodium chloride particles ($\sim 10^6/cm^{-3}$) were generated by a particle generator and then collected on the nano-film detectors for a certain time period (*e.g.* 30 min, 45 min and 60 min) using an electrostatic precipitator (ESP) with a flow rate of 0.3 L/min. In theoretical calculation, the coverage percentage was around 5 - 20%. Detectors with different collection times were scanned by an AFM. The specific coverage percentages for each detector were determined through a function in the software of the AFM called bearing analysis. In the analysis, all the bumps (particles) above the surface of the nano-film were included to determine the coverage percentages. Fig. 4 presents deposited ultrafine particles on the coated QCM detectors under different coverage percentages. All the particles above the surface were marked in blue. From upper left to lower right panels, the coverage percentages were 3%, 5%, 10% and 13%, respectively. It was found that particles were well separated at low coverage percentages (*i.e.* 3%, 5% and 10%), while particles stacking appeared (inside the circle in green) at high coverage percentage of 13% (Fig. 4). Therefore, to definitely avoid particles stacking, the coverage percentage should not be higher than 10% during field measurements. Based on the concentrations of UFPs we measured at the same site in previous study (Wang et al., 2014) and preliminary calculations, it would need more than 30 days for a 10% coverage percentage of particles on the surface of a detector. Hence, 2-3 days sampling duration for

each sample collected by the QCM+DS system in ambient air would be workable. Under such conditions, sufficient frequency change was able to be obtained while particles stacking would not occur.

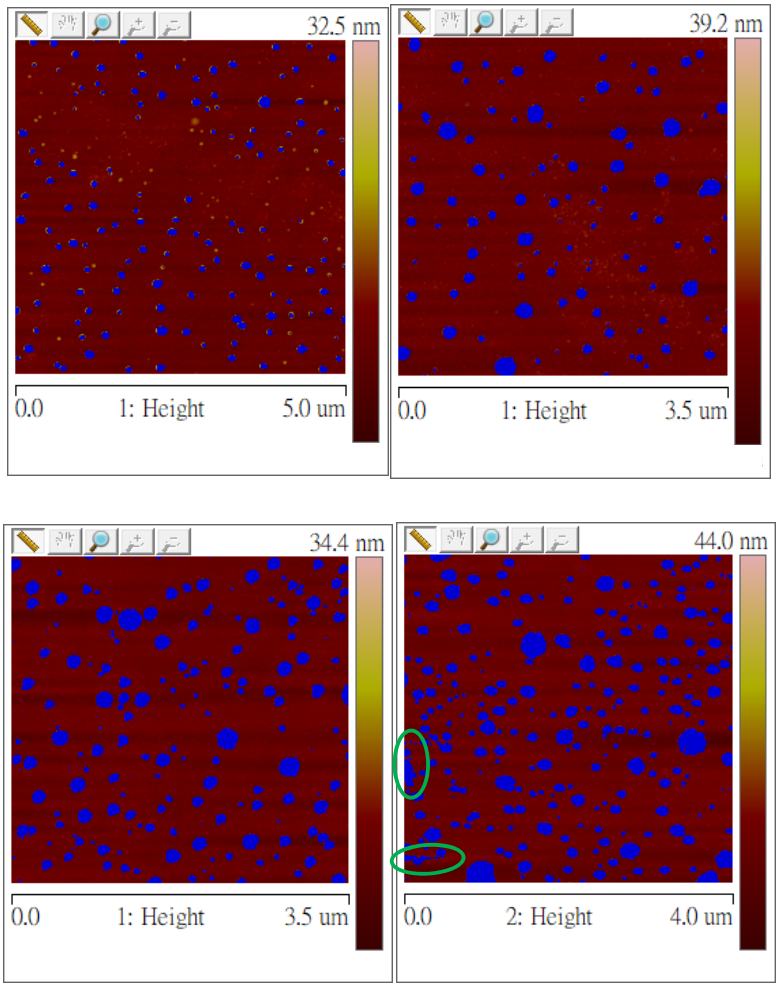

Fig. 4 Deposition of ultrafine particles under different coverage percentages. Upper left panel: 3%; upper right panel: 5%; lower left panel: 10%; and lower right panel: 13%

3.3 Removal of non-acidic particles

To remove non-acidic particles on the surface, coated detectors were put into ethanol solution for the ultrasonic for 30 mins after collection of non-acidic particles (*i.e.* NaCl particles) and acidic particles. The workability of ultrasonic method and its removal efficiency were examined through AFM scanning. In the scans of AFM, acidic particles were distinguished by unique reaction spots that had a central elevation with a surrounding yellow halo on the surface of the detectors, while non-acidic

particles did not have such characteristics (Wang et al., 2012). Detectors having non-acidic and acidic particles before and after the ultrasonic treatment are shown in Fig. 5 and Fig. 6, respectively. Clearly, non-acidic particles were all removed from the surface while acidic particles remained on the surface. Noteworthily, similar number of acidic particles was counted before and after the ultrasonic process in the same scanning area of AFM images.

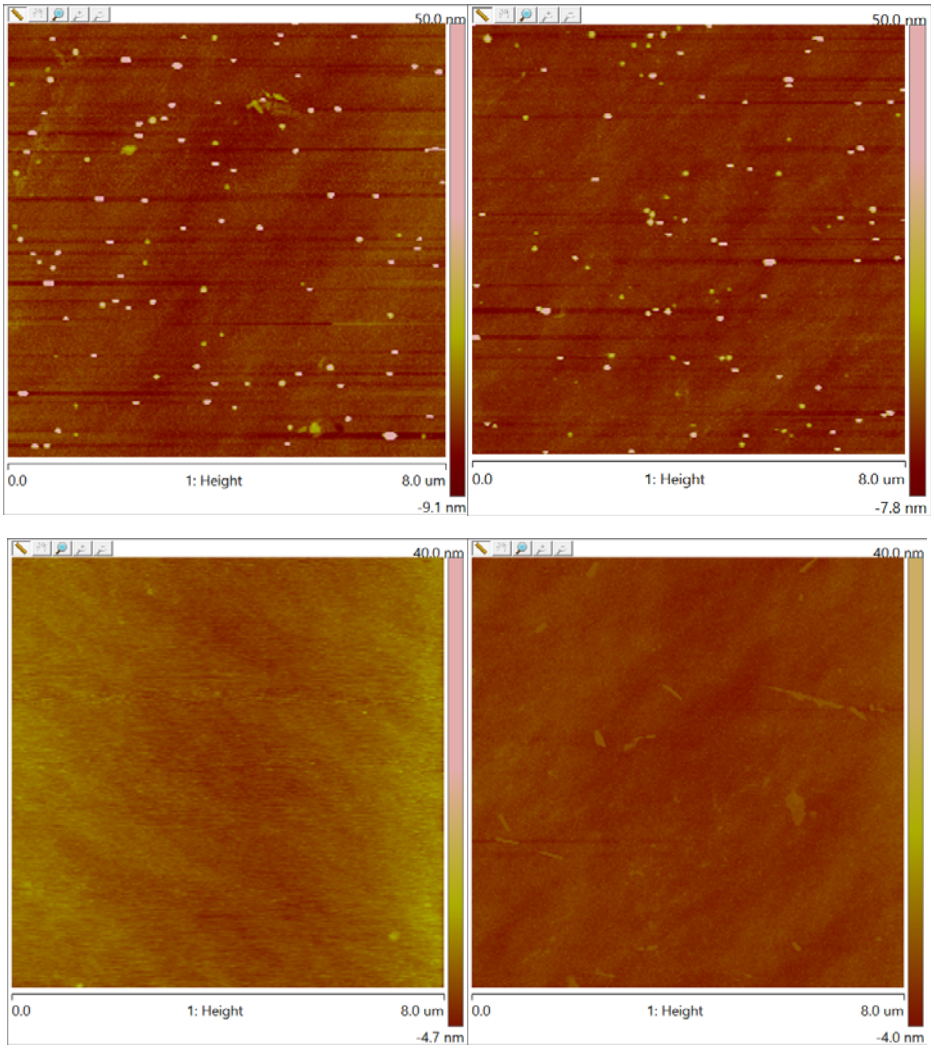

Fig. 5 AFM images of NaCl particles before (upper two panels) and after (lower two panels) ultrasonic treatment by ethanol

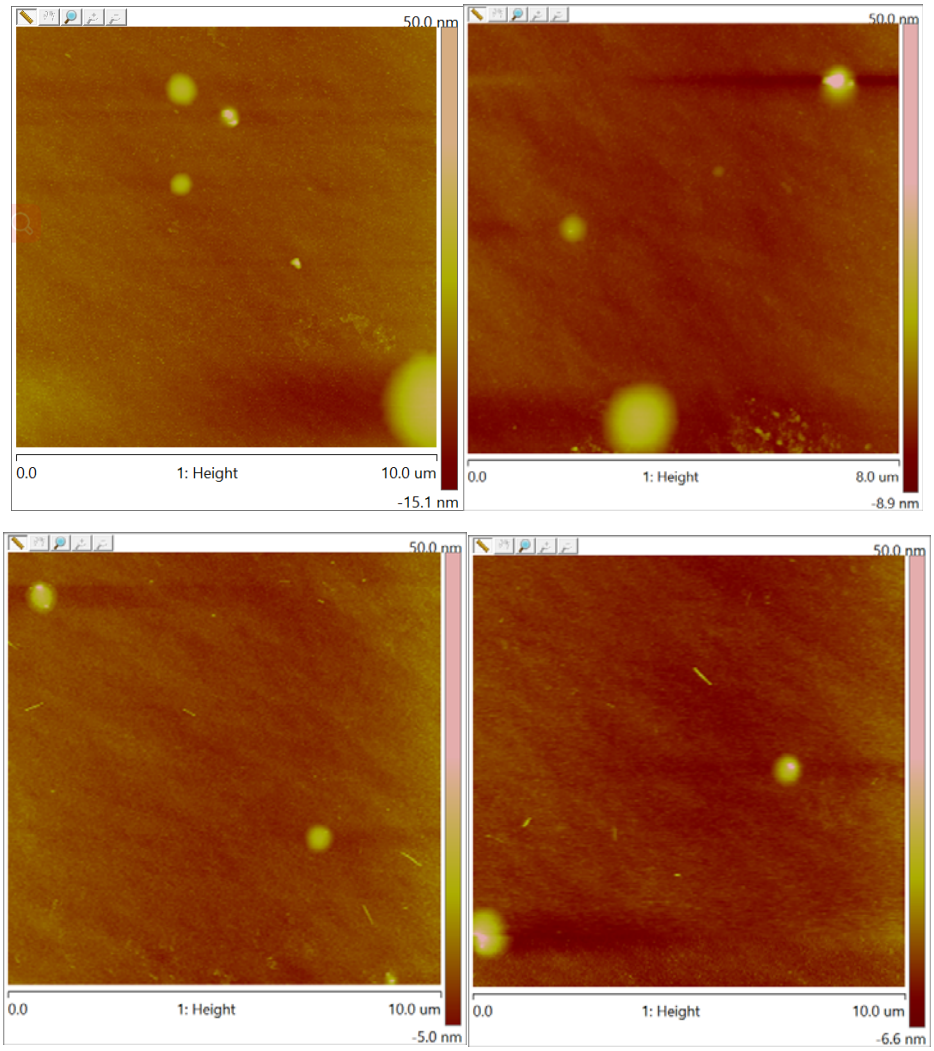

Fig. 6 AFM images of standard acidic particles before (upper two panels) and after (lower two panels) ultrasonic treatment by ethanol

Moreover, verification was conducted using the modified QCM+DS system. Both standard acidic and non-acidic particles were generated and collected on the metal-QCM detectors. After a certain reaction time (more than one day), the detectors having non-acidic and acidic particles on the surface were ultrasonically cleaned with ethanol for 30 min., respectively. The frequencies of the metal-QCM detector before and after ultrasonic treatment were obtained. It was found that the frequency of the metal-QCM detector with acidic particles remained almost unchanged after 30 min. of ultrasonic cleaning (*i.e.* frequency change < 0.1 Hz), revealing that acidic particles were unable to be removed by ultrasonic cleaning. Instead, ultrasonic treatment of the detector with non-acidic particles caused

frequency enhancement, opposite to the frequency reduction caused by the mass of deposited particles, suggesting that non-acidic particles were removed during the ultrasonic process. In summary, ultrasonic treatment with ethanol effectively removed non-acidic particles on the surface of the metal-QCM detectors while retaining acidic particles.

3.4 Collection efficiencies of the QCM+DS system

Fig. 7 illustrates the collection efficiencies of the QCM+DS system at different flow rates for different sizes of particles. Obviously, all the stepwise collection efficiencies in the QCM+DS system deceased with the increase of flow rate, regardless of particle size, probably owing to the fact that the deposition positions of the particles were beyond the sampling spots inside the system after the increase of flow rate. It also implied that there was a significant dependence of diffusion deposition on the flow rate. In addition, the collection efficiencies on small particles were higher than those on large particles when the flow rate was the same, consistent with the theory of diffusion deposition, suggesting that the deposition of particles in the QCM+DS system obeyed the principle of diffusion deposition (Hinds, 1999; Wang et al., 2014). The relationships between the experimentally-determined collection efficiencies and deposition parameters were determined by multivariate nonlinear regression analysis (Origin Pro 2017, USA).

Specifically, at the sampling spot A (Fig. 1), the values of deposition parameter (μ) for most experimental scenarios were smaller than 0.003. According to our previous study, the collection efficiency (η_a) had a power–law relationship with μ (Wang et al., 2014). Thus, the collection efficiency as a function of μ was estimated from the 12 experimental scenarios by a model: $\eta_a = \alpha_1 \times (\mu_2^{\alpha 2} - \mu_1^{\alpha 2})$ using the Quasi-Newton method. The μ_1 and μ_2 are the independent variables. The two parameters α_1 and α_2 are constants. After model simulations, the semi-empirical equation for the diffusive collection efficiency at the sampling spot A was obtained as follows (Eq. 9):

$$\eta_a = 20.532 \times (\mu_2^{0.671} - \mu_1^{0.671}) \qquad \text{Eq. 9}$$

where μ_1 and μ_2 represent the deposition parameters at the starting and ending points of sampling spot A (*i.e.* 8.14 cm and 8.86 cm, respectively), and are calculated using Eq. 4 and Eq. 5; the constant α_1 is a modified factor and α_2 is a power-law exponent obtained from experimental data, which are 20.532

and 0.671 (regression coefficient r = 0.914) in Eq. 9, respectively.

However, at the sampling spots B and C, the relationships between collection efficiencies (η_b and η_c) and μ were different. On one hand, most values of μ at the two sampling spots were larger than 0.003, except for large particles (*e.g.* > 200 nm) at high sampling flow rate (*e.g.* > 0.5 l/min) at sampling spot B, indicating that there was an exponential relationship of μ with η_b and η_c according to the theory of diffusion deposition (Hinds, 1999). On the other hand, the calibrated collection efficiency did not show a power-law function with the sampling flow rate for every size of particles at these two sampling spots in the previous DS (Wang et al., 2014). Therefore, different exponential models (*i.e.* $\eta_b = \beta_1 \times [\exp(\beta_2 \times \mu_3) - \exp(\beta_2 \times \mu_4)]$ and $\eta_c = \gamma_1 \times [\exp(\gamma_2 \times \mu_5) - \exp(\gamma_2 \times \mu_6)]$) were adopted to determine the η_b and η_c as a function of μ by multivariate nonlinear regression method. The constant β_1 and γ_1 were the modified factors for the semi-empirical equations; β_2 and γ_2 were the determined constants for the independent variables at the sampling spots B and C, respectively. By fitting the 12 experimental scenarios at each sampling spot into the two models, the semi-empirical equations for the diffusive collection efficiency at the sampling spots B and C (*i.e.* η_b and η_c) were obtained (Eq. 10 and Eq. 11), respectively:

$$\eta_b = 7.435 \times [\exp(-20.132 \times \mu_3) - \exp(-20.132 \times \mu_4)] \quad \text{Eq. 10}$$

$$\eta_c = -11.253 \times [\exp(7.520 \times \mu_5) - \exp(7.520 \times \mu_6)] \quad \text{Eq. 11}$$

where μ_3, μ_4, μ_5 and μ_6 represent the deposition parameters at the starting and ending points of sampling spots B (19.79 cm and 20.51 cm) and C (46.89 cm and 47.61 cm), respectively; constants β_1 and β_2 are 7.435 and -20.132 (r = 0.959) for the collection efficiency of sampling spot B, respectively (Eq. 10); and γ_1 and γ_2 are -11.253 and 7.520 (r = 0.971) for the collection efficiency of the sampling spot C, respectively (Eq. 11).

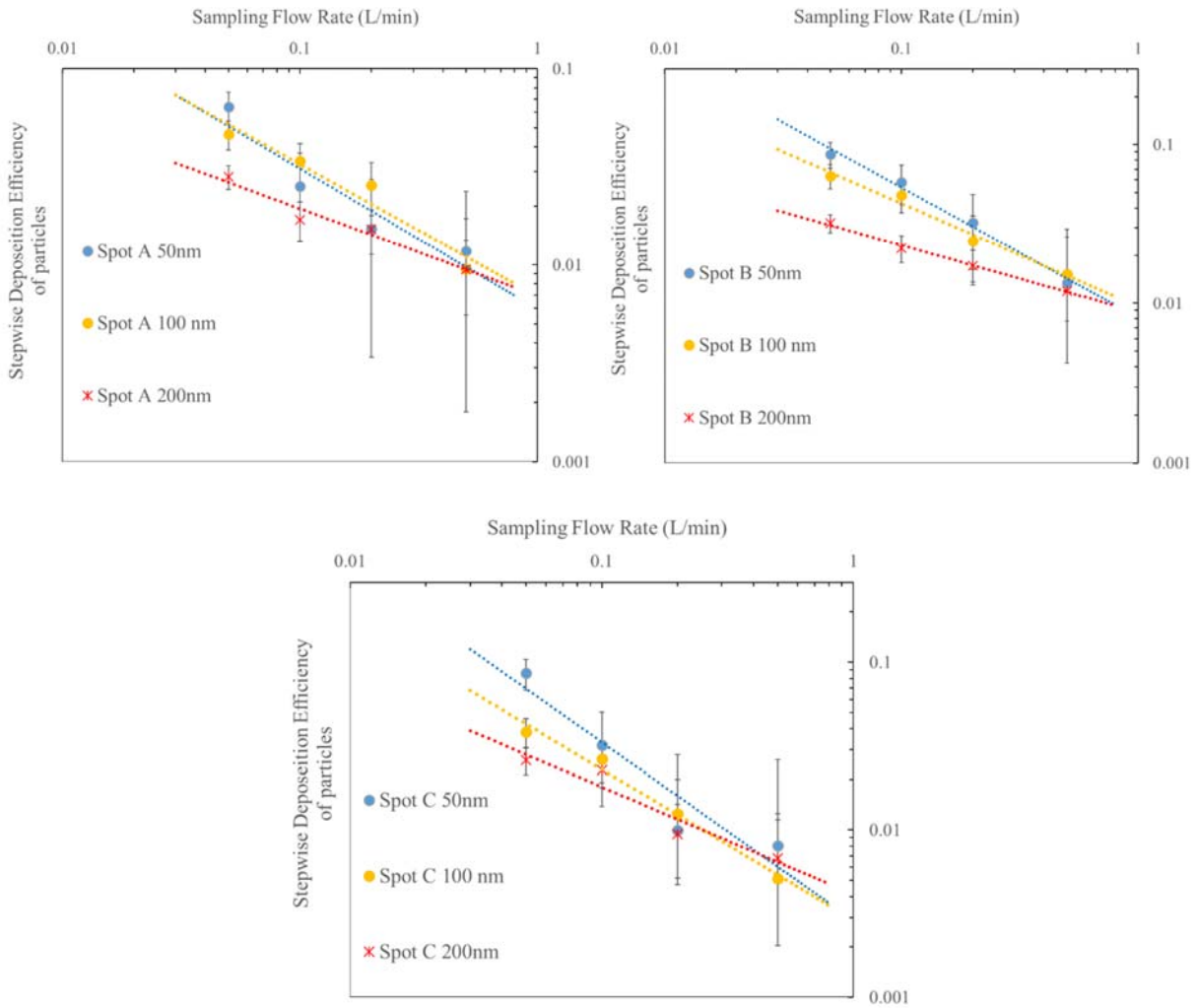

Fig. 7 Collection efficiencies of the QCM+DS system at the sampling spot A (upper left), spot B (upper right) and spot C (lower) at four different flow rates for three different sizes of particles

3.5 Validation via a field measurement

Table 1 lists the concentrations of AUFPs and total UFPs measured by the QCM+DS system on 11-13 April 2019 as an example. The mass concentrations of UFPs in spots A, B and C were 5.03, 2.85 and 6.49 μg/m^3, respectively. By considering the proportion of AUFPs in UFPs through the removal process of non-AUFPs, the mass concentrations of AUFPs were further determined to be 1.07, 0.74 and 0.97 μg/m^3 at spots A, B and C, respectively. Number concentrations of UFPs and AUFPs were estimated by converting mass concentrations using the assumed density of particles (i.e. 2.5 g/cm^3) (Ferro et al., 2004; Cha and Olofsson, 2018). Noteworthily, although the mass concentrations of UFPs

and AUFPs measured at spot B were the lowest among the three sampling spots, the number concentrations were the highest. These were mainly caused by the higher mass concentrations of smaller sizes of particles (i.e. 5.5 nm -17 nm) measured at spot B than those at spots A and C, which significantly enhanced the calculated total particle number and thus led to high number concentrations. Eventually, the values at sampling spots A, B and C were averaged and regarded as the average concentrations of UFPs and AUFPs on these days.

473 Table 1 Concentrations of AUFPs and total UFPs measured by the QCM+DS system on 11-13 April, 2019

Data & Time	*Sampling Spot*	*Particle size bin (nm)*	*Frequency change (Hz)*	*Total mass of particles in the sample air (μg)*	*Estimated total number of particles in the sample air*	*Proportion of AUFPs in UFPs (%)*	*Mass concentration of UFPs ($\mu g/m^3$)*	*Number concentration of UFPs (cm^{-3})*	*Mass concentration of AUFPs ($\mu g/m^3$)*	*Number concentration of AUFPs (cm^{-3})*
11-13 April 2019	Spot A	124~150	1.72	0.79	2.24×10^8	21.2	5.03	1.16×10^4	1.07	2.44×10^3
		75~112	1.09	0.37	4.35×10^8					
		47~69	0.53	0.11	5.04×10^8					
		30~43	0.31	0.03	5.11×10^8					
		19~27	0.22	0.02	8.61×10^8					
		5.5~17	0.12	0.003	5.38×10^8					
	Spot B	124~150	1.10	0.39	1.09×10^8	26.3	2.85	2.10×10^4	0.74	5.47×10^3
		75~112	0.72	0.23	2.76×10^8					
		47~69	0.57	0.08	3.54×10^8					
		30~43	0.22	0.02	2.94×10^8					
		19~27	0.17	0.01	6.65×10^8					
		5.5~17	0.16	0.02	3.86×10^9					
	Spot C	124~150	0.98	1.13	3.20×10^8	15.7	6.49	1.59×10^4	0.97	2.39×10^3
		75~112	0.77	0.41	4.92×10^8					
		47~69	0.42	0.10	4.34×10^8					
		30~43	0.40	0.04	6.69×10^8					
		19~27	0.49	0.02	1.04×10^9					
		5.5~17	0.36	0.01	1.25×10^9					

Table 2 Comparisons of concentrations of AUFPs and total UFPs measured by the QCM+DS system, the SMPS and the previous DS+AFM system

Date	***SMPS***		***Previous DS+AFM***				***QCM+DS***			
	Number concentration of UFPs $\times10^4$ (cm^{-3})	Estimated mass concentration of UFPs ($\mu g/m^3$)	Number concentration of UFPs $\times10^4$ (cm^{-3})	Estimated mass concentration of UFPs ($\mu g/m^3$)	Number concentration of AUFPs$\times10^3$ (cm^{-3})	Estimated mass concentration of AUFPs ($\mu g/m^3$)	Mass concentration of UFPs ($\mu g/m^3$)	Estimated number concentration of UFPs $\times10^4$ (cm^{-3})	Mass concentration of AUFPs ($\mu g/m^3$)	Estimated number concentration of AUFPs $\times10^3$ (cm^{-3})
11-13 April 2019	0.86±0.39	3.14±1.16	1.69±0.38	2.22±0.50	0.96±0.53	0.13±0.07	4.79±1.68	1.62±0.43	0.93±0.15	3.43±1.62
13-15 April 2019	0.91±0.38	4.84±2.34					4.65±3.00	1.42±0.51	0.84±0.35	2.79±0.71
15-17 April 2019	1.27±0.57	4.28±1.92	2.00±0.31	2.61±0.40	3.01±1.23	0.39±0.16	4.82±3.41	1.32±0.56	0.88±0.54	2.52±0.53
23-25 April 2019	0.67±0.32	2.86±1.27	1.71±0.81	2.24±1.06	1.16±0.78	0.15±0.10	2.88±1.26	0.92±0.11	0.56±0.21	1.94±0.74

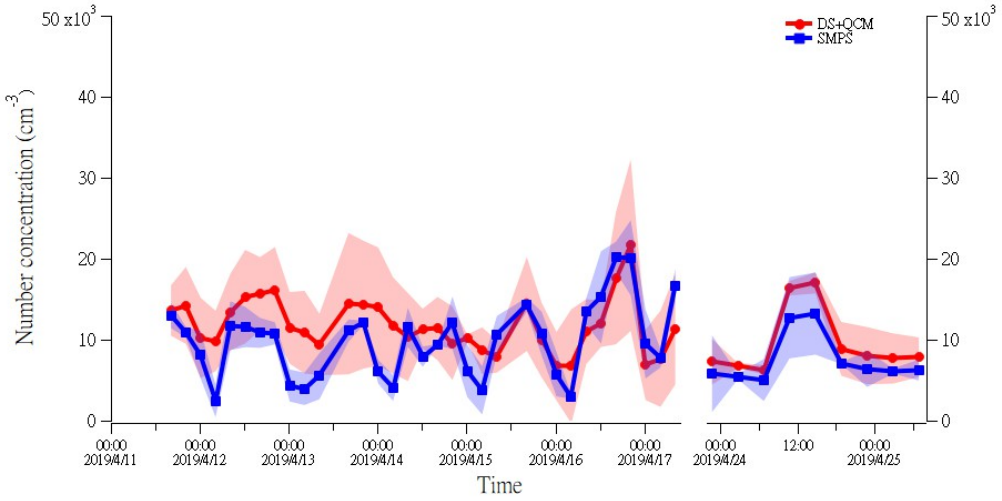

Fig. 8 Temporal variations of number concentrations of UFPs measured by QCM+DS system and SMPS on 11-25 April 2019

Table 2 compares the results of SMPS, previous DS+AFM and the QCM+DS system from the field measurement. Note, only one set of detectors was collected on 11-15 April using the previous DS given the levels of particles on these days and the sensitivity of the previous DS detectors. The average UFP number concentrations and mass concentrations measured by the QCM+DS system were in line with those measured by previous DS+AFM method ($p > 0.05$) and SMPS ($p > 0.05$), implying the consistency of the QCM+DS system. To further evaluate the performance of the QCM+DS system, the temporal variations of UFP number concentrations measured by the QCM+DS system and the SMPS on 11-25 April 2019 are shown in Fig. 8. Concentrations of UFPs measured by the QCM+DS system and the SMPS were both acquired and compared at a 4-hours interval. Overall, the temporal variation trends of the UFP concentrations measured by both methods were similar with a good index of agreement (IOA = 0.77), which again indicated the consistency of results from both methods. Low levels of UFPs were usually found at night, while high UFP concentrations were observed at daytime hours, in agreement with the pattern of human activities. The discrepancy of results was mainly attributed to two factors. On one hand, the QCM+DS system estimated the UFP number concentrations based on the density of UFPs reported in previous study, which might cause uncertainties. On the other hand, the QCM+DS system was not as sensitive as the SMPS, not only in time-resolution but also in size-resolution, which likewise led to a certain degree of uncertainty in determining UFP concentrations. Specifically, SMPS measured the particle concentration every 10s for a specific size, while the QCM+DS system acquired the particle concentration in a size bin every 15 mins. To achieve a higher time-resolution and/or size-resolution, improvements could be made by replacing the 5 MHz QCM detector in the study to a more sensitive QCM detector (e.g. 10 MHz, 20 MHz and 50 MHz QCM detectors) (Pohanka, 2017).

As for the concentrations of AUFPs, only the data obtained from the previous DS+AFM method and the QCM+DS system were compared since the SMPS was unable to measure the AUFP concentrations (Table 2). Generally, the AUFP concentrations measured by the QCM+DS system were higher than those measured by the previous DS+AFM method. Difference was significant in mass concentration ($p < 0.05$) but not obvious in number concentration ($p > 0.05$). In addition to the impact of assumed particle density, the difference may be caused by the random selection of the AFM scanning areas in

the DS+AFM method and the measurement deviation of the QCM system. The proportions of AUFPs in UFPs (DS+AFM: 10.1% ± 5.2% and QCM+DS: 20.3% ± 7.0%) were significantly decreased compared to those measured in 2010 (DS+AFM: 44.9%±8.6%) at the same site regardless of methods (both $p < 0.05$), while the number concentrations of UFPs were comparable to those observed in 2010 ($p > 0.05$) (Wang et al., 2014). The decreased levels of AUFPs in this study against those in 2010 implied effective control of SO_2 which is the precursor of acidic particles (i.e. sulfuric and hydrogen sulfate). Indeed, SO_2 levels in Hong Kong and adjacent inland Pearl River Delta region from 2010 to 2019 have been significantly reduced by 55.4% and 63.0%, respectively, reported by the Hong Kong Environmental Protection Department (https://www.epd.gov.hk/epd/tc_chi/resources_pub/publications/m_report.html). Compared with the proportion measured by the QCM+DS, the lower proportion of AUFPs in UFPs obtained by the DS+AFM method might be underestimated due to the uncertainties in the selection of the AFM scanning areas, especially when the concentrations of AUFPs in the atmosphere were low.

Overall, based on comparison with the results of SMPS and previous DS + AFM methods, the QCM+DS system was satisfactory for the measurements of UFPs and AUFPs. Compared to the previous method (DS+AFM), the QCM+DS system abandoned a time-consuming and complicated instrument (*i.e.* AFM) and developed from an offline method to a semi-online method. The DS + AFM method required about one day to scan one set of samples (Wang et al., 2014), while the QCM+DS system used to measure UFPs had a time resolution of two hours. Moreover, the large size (60cm×60cm×80cm) and heavy weight (~ 100 kg) made the AFM difficult to be widely used in the field measurements. Without an AFM, the QCM+DS system was miniature (50cm×20cm×30cm; 15kg). Overall, the QCM+DS method was portable, compact and user-friendly. Nevertheless, time-resolution and/or size-resolution of the QCM+DS system could be further improved. At this stage, it takes two days of sampling time to gain the concentration of AUFPs. Furthermore, the QCM + DS system cannot be used to obtain the size distribution of AUFPs. Both are challenges for the development of methods for measuring AUFPs in the atmosphere in future study.

4. Summary and Conclusions

In this study, a QCM+DS method was developed to semi-automatically determine the concentrations

of ambient AUFPs and UFPs, based on the diffusion deposition of ultrafine particles in a diffusion sampler and the online detection of the mass of UFPs using a metal-QCM detector. The QCM+DS method was accomplished by combining the previous DS and three QCM systems. Modifications were made to the inlet of the sampler and the sampling spots inside the sampler to collect size-resolved particles and place detectors inside the sampler, respectively. Furthermore, the QCM detector was altered by coating a nano-metal film on its surface using a magnetron sputtering system to generate a metal-QCM detector for collecting and identifying AUFPs. According to the different attraction of AUFPs and non-acidic UFPs to metal film, ultrasonic treatment by ethanol removed the non-acidic particles on the surface of the detector, while retaining the acidic particles. AUFPs were identified and quantified based on the frequency change of the metal-QCM detectors during ultrasonic processing and sampling. Prior to field measurements for method validation, calibration experiments were conducted to determine the sensitivity factor of the modified QCM detector and the relationship of collection efficiency with particle size and sampling flow rate in the QCM+DS system.

In the field sampling campaigns, the total UFPs number and mass concentrations measured by the QCM+DS system showed fairly good agreements with the results of the other two methods (i.e. SMPS and DS+AFM). In addition, the concentrations of AUFPs measured by the DS+AFM system were lower than those obtained by the QCM+DS method, which might be caused by underestimation of the DS+AFM method due to the uncertainties in the selection of the AFM scanning areas. The difference between these two methods was significant in mass concentration but insignificant in number concentration. In short, the QCM+DS system is satisfactory and reliable for the measurements of ambient UFPs and AUFPs. Improvements can be further made by increasing the time-resolution and/or size-resolution of the method and obtaining the size distribution of AUFPs.

Acknowledgements

This study was supported by the Strategic Focus Area scheme of The Research Institute for Sustainable Urban Development at The Hong Kong Polytechnic University (1-BBW9), the Environment and Conservation Fund (ECF) of the Hong Kong Special Administrative Region (ECF59/2015) and the Hong Kong PhD Fellowship (Project Number: RULW).

543 **References**

544 Arouca, F. O., Feitosa, N. R., and Coury, J. R. 2010. Effect of Sampling in the Evaluation of Particle
545 Size Distribution in Nanoaerosols. *Powder technology*, *200*(1-2), 52-59.

546 Binks, B. P., and Olusanya, S. O. 2017. Pickering Emulsions Stabilized by Coloured Organic Pigment
547 Particles. *Chemical science*, *8*(1), 708-723.

548 Buttry, D. A. 1991. Applications of the Quartz Crystal Microbalance to Electrochemistry.
549 *Electroanalytical Chemistry: A Series of Advances,* In: Bard, A. J. (Ed.), Vol 17, Marcel Dekker, New
550 York, 1-85.

551 Cohen, B. S., Li, W., Xiong, J. Q., and Lippmann, M. 2000. Detecting H^+ in Ultrafine Ambient Aerosol
552 using Iron Nano-Film Detectors and Scanning Probe Microscopy. *Applied Occupational and*
553 *Environmental Hygiene*, *15*, 80-89.

554 Cohen, B. S., Heikkinen, M. S., and Hazi, Y. 2004. Airborne Fine and Ultrafine Particles Near the
555 World Trade Center Disaster Site. *Aerosol science and technology*, *38*(4), 338-348.

556 Cha, Y., and Olofsson, U. 2018. Effective Density of Airborne Particles in a Railway Tunnel from Field
557 Measurements of Mobility and Aerodynamic Size Distributions. *Aerosol Science and*
558 *Technology*, *52*(8), 886-899.

559 Chen, M., Romay, F. J., Li, L., Naqwi, A., and Marple, V. A. 2016. A Novel Quartz Crystal Cascade
560 Impactor for Real-Time Aerosol Mass Distribution Measurement. *Aerosol Science and*
561 *Technology*, *50*(9), 971-983.

562 Ferro, A. R., Kopperud, R. J., and Hildemann, L. M. 2004. Elevated Personal Exposure to Particulate
563 Matter from Human Activities in a Residence. *Journal of Exposure Science and Environmental*
564 *Epidemiology*, *14*(1), S34-S40.

565 Franken, R., Maggos, T., Stamatelopoulou, A., Loh, M., Kuijpers, E., Bartzis, J., et al. 2019.
566 Comparison of Methods for Converting Dylos Particle Number Concentrations to PM2.5 Mass
567 Concentrations. *Indoor air*, *29*(3), 450-459.

568 Gilmour, P. S., Ziesenis, A., Morrison, E. R., Vickers, M. A., Drost, E. M., Ford, I., et al. 2004.

569 Pulmonary and Systemic Effects of Short-Term Inhalation Exposure to Ultrafine Carbon Black
570 Particles. *Toxicology and Applied Pharmacology*, *195*(1), 35-44.

571 Hinds, W. C. 1999. Properties, behavior, and measurement of airborne particles. *Aerosol Technology,*
572 *2nd ed,* John Wiley and Sons Press, New York, 182-204.

573 Heath, G. R., and Scheuring, S. 2018. High-speed AFM Height Spectroscopy Reveals μs-Dynamics
574 of Unlabeled Biomolecules. *Nature communications*, *9*(1), 1-11.

575 Kim, Y. P., Pun, B., Chan, C. K., Flagan, R. C., and Seinfeld, J. H. 1994. Determination of Water
576 Activity in Ammonium Sulfate and Sulfuric Acid Mixtures Using Levitated Single Particles.
577 *Environmental Science and Technology*, *20*, 275-284.

578 Li, Y. J., Cheong, G., Lau, A. P. S., and Chan, C. K. 2010. Acid-Catalyzed Particle-Phase Reactions of
579 Limonene and Terpineol and Their Impacts on Gas-to-Particle Partitioning in the Formation of Organic
580 Aerosols. *Environmental Science and Technology*, *44*, 5483-5489.

581 Lippmann, M., and Thurston, G. D. 1996. Sulfate Concentrations as an Indicator of Ambient
582 Particulate Matter Air Pollution for Health Risk Evaluations. *Journal of Exposure Analysis and*
583 *Environmental Epidemiology*, *6*(2), 123-146.

584 McCallum, J. J. 1989. Piezoelectric Devices for Mass and Chemical Measurements: An Update.
585 *Analyst*, *114*, 1173.

586 Peters, A., Dockery, D. W., Heinrich, J., and Wichmann, H. E. 1997. Short-Term Effects of Particulate
587 Air Pollution on Respiratory Morbidity in Asthmatic Children. *European Respiratory Journal*, *10*,
588 872-879.

589 Pohanka, M. 2017. The Piezoelectric Biosensors: Principles and Applications. *International Journal*
590 *of Electrochemical Science*, *12*, 496-506.

591 Sarangi, B., Aggarwal, S. G., Sinha, D., and Gupta, P. K. 2016. Aerosol Effective Density Measurement
592 using Scanning Mobility Particle Sizer and Quartz Crystal Microbalance with the Estimation of
593 Involved Uncertainty. *Atmospheric Measurement Techniques*, *9*(3), 859-875.

594 Shrivastava, A., and Gupta, V. B. 2011. Methods for the Determination of Limit of Detection and Limit

of Quantitation of the Analytical Methods. *Chronicles of young scientists*, *2*(1), 21.

Thurston, G. D., Ito, K., Hayes, C. G., Bates, D. V., and Lippmann, M. 1994. Respiratory Hospital Admissions and Summertime Haze Air Pollution in Toronto, Ontario: Consideration of the Role of Acid Aerosols. *Environmental Research*, *65*, 271-290.

Thurston, G. D., Ito, K., Kinney, P. L., and Lippmann, M. 1992. A Multi-Year Study of Air Pollution and Respiratory Hospital Admissions in Three New York State Metropolitan Areas: Results for 1988 and 1989 Summers. *Journal of Exposure Analysis and Environmental Epidemiology*, *2*, 429-450.

Thurston, G. D., Ito, K., Lippmann, M., and Hayes, C. G. 1989. Re-examination of London Mortality in Relation to Exposure to Acidic Aerosols During 1962-1973 Winters. *Environmental Health Perspectives*, *79*, 73-82.

Wang, D. W., Guo, H., and Chan, C. K. 2014. Diffusion Sampler for Measurement of Acidic Ultrafine Particles in the Atmosphere. *Aerosol Science and Technology*, *48*(12), 1236-1246.

Wang, D. W., Guo, H., and Chan, C. K. 2012. Measuring Ambient Acidic Ultrafine Particles Using Iron Nanofilm Detectors: Method Development. *Aerosol Science and Technology*, *46*, 521-532.

Wang, J., Zhu, J., and Liew, P. J. 2019. Material Removal in Ultrasonic Abrasive Polishing of Additive Manufactured Components. *Applied Sciences*, *9*(24), 5359.

Ward, M. D., and Buttry, D. A. 1990. In-situ Interfacial Mass Detection with Piezoelectric Transducers. *Science*, *249*, 1000.

Wichmann, H. E., Spix, C., Tuch, T., Wolke, G., Peters, A., Heinrich, J., Kreyling, W. G., and Heyder, J. 2000. Daily Mortality and Fine and Ultrafine Particles in Erfurt, Germany Part I: Role of Particle Number and Particle Mass. *Research Report (Health Effects Institute)*, (*98*), 5-86.

Zhang, R.Y., Alexei, F. K., Joakim, P., Zhang, D., Xue, H. X., and McMurry, P. H. 2008. Variability in Morphology, Hygroscopicity, and Optical Properties of Soot Aerosols During Atmospheric Processing. *Proceedings of the National Academy of Sciences of the United States of America*, *30*, 10291-10296.